STM JOURNALS

International Journal of
Biomedical Innovations
and Engineering

Volume 2, Issue 1, 2024
January–June
DOI (Journal): 10.37591/IJBIE

https://journals.stmjournals.com/ijbie

Research IJBIE

Development of an Innovative Nanotransdermal Formulation Utilizing an Optimal Combination of Acyclovir and Omeprazole to Improve Antiviral Efficacy

E. Sri Divya[1,*], Nansri Saha[2]

Abstract

The study effectively created nanogel formulations of Acyclovir and Omeprazole using the solvent diffusion technique. Among the various formulations (F1–F9), F9 was identified as the most suitable for gel preparation based on its pH evaluation. Drug content analysis, performed using UV-spectroscopy, confirmed the homogeneity of the prepared nanogels, which appeared opaque, free of lumps, particles, or aggregates. The spreadability assessment of F9 demonstrated excellent spreadability, while viscosity values for all formulations ranged between 3268 and 3528 cps, indicating stability. The in-vitro dissolution tests showed that formulation F9 demonstrated a significantly improved rate of dissolution. Further characterization of F9 showed a particle size of 687.4 nm, a PDI of 0.842, and a zeta potential of -43.7 mV. TEM imaging confirmed the spherical shape and smooth surface of the particles, with sizes around 650 nm. A comparative in-vitro release study between the F9 nanogel and the marketed acyclovir formulation (MF) demonstrated that the nanogel provided sustained drug release and superior antiviral activity. This indicates that transforming Acyclovir and Omeprazole into a nanogel formulation significantly enhances their therapeutic efficacy compared to conventional formulations.

Keywords: Formulation, nano transdermal, acyclovir, omeprazole, anti-viral activity

INTRODUCTION

Transdermal drug delivery is a patient-friendly and minimally invasive approach to administering therapeutic substances. This approach not only enhances medication bioavailability by targeting specific skin areas but also reduces the likelihood of unexpected side effects. Transdermal drug delivery has garnered considerable interest as a non-invasive alternative to oral administration and hypodermic injections. This method offers several advantages, including improved bioavailability by bypassing the first-pass metabolism in the liver, sustained and controlled release of medication, and enhanced patient compliance due to its ease of use and reduced dosing frequency. Additionally, transdermal systems can minimize gastrointestinal side effects and provide a steady plasma concentration of the drug, making them a compelling option for various therapeutic applications. The FDA first approved transdermal

Author for Correspondence
E.sri Divya
E-mail: sridivya7284@gmail.com

[1]Student, Department of Pharmaceutics, SSJ College of Pharmacy, Hyderabad, Telangana, India
[2]Associate Professor, Department of Pharmaceutics, SSJ College of Pharmacy, Hyderabad, Telangana, India

Received Date: February 08, 2024
Accepted Date: February 11, 2024
Published Date: February 29, 2024

Citation: E. Sri Divya, Nansri Saha. Development of an Innovative Nanotransdermal Formulation Utilizing an Optimal Combination of Acyclovir and Omeprazole to Improve Antiviral Efficacy. International Journal of Biomedical Innovations and Engineering. 2024; 2(1): 19–35p.

patches in the 1970s for delivering scopolamine to treat motion sickness. Since then, extensive advancements have been made in transdermal drug delivery systems (TDDs) using both physical and chemical strategies.

Physical methods include techniques such as epidermal erosion, skin puncture devices, microneedle arrays, high-frequency oscillating needle bundles, and high-velocity dry powder jets. Chemical methods involve penetration enhancers and prodrugs. However, both approaches have limitations. Physical methods, like iontophoresis, can cause discomfort, including pain, burning sensations, blistering, or even skin necrosis if the current is too strong or applied for prolonged periods. Sonophoresis may lead to mild itching, irritation, and burning, while microneedles can trigger skin allergies or irritation, particularly in sensitive individuals.

On the other hand, chemical approaches such as topical formulations (creams, gels, ointments, and oils) often suffer from poor permeation through the stratum corneum (SC), requiring higher doses and frequent application. This can lead to adverse effects like skin rashes and itching, significantly reducing patient compliance for long-term treatments. Prodrugs, while useful in overcoming skin barriers, may release redundant byproducts that could cause harmful effects.

Consequently, there is a pressing need to develop innovative TDDs that enhance drug penetration through the skin barrier, ensuring effective therapeutic concentrations in target tissues without compromising patient safety or comfort.

Transdermal drug delivery is a patient-friendly and minimally invasive technique for administering therapeutic agents. This method improves medication bioavailability by targeting specific areas of the skin while minimizing the risk of unexpected side effects. As a promising alternative to oral medications and hypodermic injections, transdermal delivery has gained considerable attention. The FDA first approved transdermal patches in the 1970s for administering scopolamine to combat motion sickness, marking the beginning of significant advancements in transdermal drug delivery systems (TDDs) through physical and chemical approaches.

Physical methods include techniques like epidermal abrasion, skin puncture devices, microneedle arrays, high-frequency oscillating needles, and high-speed dry powder jets. Chemical approaches to transdermal drug delivery often utilize penetration enhancers and prodrugs to facilitate the movement of therapeutic agents through the skin barrier. However, these methods present specific challenges. Penetration enhancers can sometimes cause skin irritation or damage, while prodrugs may introduce complexities in drug activation and potential side effects from the pro-moiety. Therefore, while effective in certain contexts, these chemical strategies require careful consideration to balance efficacy with safety. For instance, physical techniques like iontophoresis may cause discomfort, including pain, burning sensations, blistering, or even skin damage if the current intensity is too high or used for extended periods. Sonophoresis can lead to mild itching, irritation, or burning, while microneedles may provoke allergic reactions or skin irritation in sensitive individuals.

Similarly, chemical approaches such as topical formulations—creams, gels, ointments, and oils—often face difficulties in penetrating the stratum corneum (SC). This limitation requires higher doses and frequent application, which can result in side effects such as skin rashes and itching, negatively impacting long-term patient compliance. Although prodrugs can help bypass skin barriers, they often release unwanted byproducts that might cause adverse effects.

Therefore, it is essential to explore and develop advanced TDDs that enhance drug penetration through the skin, achieving therapeutic concentrations in targeted tissues without compromising patient comfort or safety.

This research aims to develop an innovative nanotransdermal formulation that combines acyclovir and omeprazole to enhance antiviral efficacy.

METHODOLOGY

Pre-formulation Studies

Pre-formulation studies focus on the physical, chemical, and biological evaluation of new drug substances to create stable, safe, and effective dosage forms. These studies provide essential data on the drug compound, serving as the foundation for developing a stable and bio-pharmaceutically appropriate dosage form, as illustrated in Table 1.

Physical Characteristics

The drug's physical characteristics—including color, odor, and texture—were assessed through visual inspection. Such organoleptic evaluations are essential in pharmacognosy for identifying and ensuring the quality of crude drugs.

Table 1. List of materials used.

S.N.	Ingredients	Vendor
1	Acyclovir	Mercury Medicare (gift sample)
2	Omeprazole	Enal drugs Pvt. Ltd (gift sample)
3	Carbopol 940	Himedia laboratories Pvt. Ltd.

Melting Point

The drug's melting point was ascertained utilizing a digital melting point apparatus, which offers precise temperature measurements and enhances the accuracy of the determination process. A capillary tube was sealed at one end using a Bunsen burner, and the drugs, acyclovir and omeprazole, were introduced through the open end. The tube was then placed in the melting point viewer, and the temperature at which the drug began to melt was recorded as its melting point.

Solubility Test

Approximately 1 mg of acyclovir and omeprazole powder was placed in a test tube to assess their solubility in ethanol, water, pH 7.4 buffer, and methanol.

Determination of λ Max

First, 10 mg of acyclovir and omeprazole was dissolved in 10 ml of pH 7.4 buffer solution using a 100 ml volumetric flask. This solution was then diluted with distilled water to reach a final volume of 100 ml, creating a stock solution (Stock A) with a concentration of 100 μg/ml. To prepare a 2 μg/ml solution, 0.2 ml of Stock A was transferred to a 10 ml volumetric flask and diluted to the mark with the same buffer. This solution was then analyzed using a double-beam UV-visible spectrophotometer over the wavelength range of 200 to 400 nm.

Standard Curve

Precisely measured 10 mg of acyclovir and omeprazole were individually dissolved in 10 ml of pH 7.4 buffer and distilled water, respectively. The solutions were diluted further with phosphate buffer (pH 7.4) in a 100 ml volumetric flask to prepare a stock solution, called Stock A, with a final concentration of 100 μg/ml. From this stock solution, concentrations ranging from 2 to 10 μg/ml were prepared by pipetting volumes between 0.2 ml and 1 ml, which were then diluted to 10 ml using the same medium. The absorbance of each sample was recorded at 252 nm and 305 nm using a double-beam UV-visible spectrophotometer. A calibration curve was generated by plotting concentration on the x-axis and absorbance on the y-axis, followed by calculating the correlation coefficient (r^2) from the data.

FT-IR Studies (Drug-Polymer Compatibility)

The compatibility between the drug and polymer was evaluated using Fourier Transform Infrared (FTIR) Spectrophotometry with the KBr pellet method. Samples were prepared by compressing them into pellets using the KBr press technique and scanned over a wavelength range of 400–4000 cm^{-1}.

FORMULATION OF ACYCLOVIR AND OMEPRAZOLE NANOGEL

Preparation of Acyclovir and Omeprazole Nanogel

The nanogel formulation of acyclovir and omeprazole was developed using the nano solvent diffusion method. The drug was accurately weighed and dissolved in ethanol and propylene glycol with continuous stirring to form the organic phase. Separately, the aqueous phase was prepared by dissolving Carbopol-940 in water under constant stirring and heating for 20 minutes on a magnetic stirrer. The drug solution was sonicated in an ultrasonic bath for 10 minutes.

Subsequently, the drug solution was added dropwise into the aqueous phase during high-speed homogenization at 6000 rpm for 30 minutes, forming an emulsion. This emulsion was further processed into nanodroplets using a homogenizer to produce an oil-in-water (o/w) emulsion. The o/w emulsion was then homogenized for 1 hour at 8000 rpm, during which triethanolamine was added with continuous stirring to convert it into a nanogel using a combination of ultrasonication and high-speed homogenization. Gel-forming polymers, including Carbopol and Tragacanth, were used individually and in combination, as detailed in Table 2.

CHARACTERIZATION OF NANOGEL

pH

The pH was measured directly using a digital pH meter (MK-IV Systronics).

Viscosity Determination

The viscosity of the formulated gels was measured using a cone and plate viscometer (Brookfield DV1 Digital Rheometer) with spindle number 7 rotating at 10 rpm.

Table 2. Formulation table of nanogel.

Formulation code	F1	F2	F3	F4	F5	F6	F7	F8	F9
Acyclovir	5	5	5	5	5	5	5	5	5
Omeprazole	160	160	160	160	160	160	160	160	160
Tracaganth	200	400	600	800	-	-	-	-	400
Carbopol	-	-	-	-	200	400	600	800	400
PPG	4	4	4	4	4	4	4	4	4
Triethanolamine	4	4	4	4	4	4	4	4	4
water	Qs	Qs	Qs	Qs	Qs	Qs	Qs	Qs	Qs

Homogeneity Test

The homogeneity of the formulations was evaluated by visually inspecting their appearance after the gels were set in their containers. To evaluate the consistency and uniformity of each gel formulation, a small sample was placed between the thumb and index finger and gently pressed. This tactile assessment helped determine the homogeneity of the gel.

Spreadability

To assess spreadability, a specific amount of gel was placed between two glass slides, and a known weight was applied on top. The time it took for the slides to separate under the weight was recorded in

seconds. This duration was then used to calculate the spreadability of each formulation using the appropriate formula:

$$S=M.L/T \quad (1)$$

Here, S represents spreadability, M is the weight attached to the upper slide, L denotes the length of the glass slide, and T is the time required for the slides to completely separate from one another.

Viscosity

The viscosity of each gel formulation was measured at 25°C using a Brookfield viscometer equipped with spindle S-96, operating at 1 rpm. Viscosity readings were recorded in centipoise (cP). Each formulation was tested three times, and the average viscosity values were calculated.

Drug Content

To analyze the drug content, ultracentrifugation was used. A nanogel sample was dissolved in 2 ml of distilled water, transferred to a centrifuge tube, and spun at 12,000 rpm for 10 minutes. Afterward, the supernatant was filtered and analyzed using a UV-visible spectrophotometer at wavelengths of 251 nm and 300 nm.

***In-vitro* Release Study**

The in vitro drug release from the gel formulations was evaluated using Franz diffusion cells equipped with cellulose acetate membranes (Sigma Aldrich), featuring a 33 mm pore size and a 3.14 cm^2 diffusion area. The membrane was positioned between the donor and receptor chambers, with the receptor chamber containing 15 ml of phosphate buffer (pH 7.4) to maintain sink conditions. A 1 g sample of the drug-loaded gel formulation was placed in the donor chamber. Every hour for 24 hours, 0.5 ml samples were taken from the receptor chamber and replaced with an equal amount of drug-free buffer. The collected samples were analyzed using a UV spectrophotometer, scanning wavelengths between 200 and 400 nm. The experiment was conducted in triplicate, and the average cumulative drug release from the three batches was calculated.

EVALUATION OF OPTIMIZED NANOGEL

Particle Size and Polydispersity Index (PDI)

The optimized nanogel's average particle size and polydispersity index (PDI) were determined at 25°C using dynamic light scattering (DLS) with a Malvern Zetasizer Nano ZS90. The samples were placed in polystyrene cuvettes, and measurements were recorded at a fixed angle.

Zeta Potential

The zeta potential of the optimized nanogel was assessed at 25°C using a Malvern Zetasizer Nano ZS90. The samples were placed in polystyrene cuvettes, and a zeta dip cell was used for the measurements.

TEM (Transmission Electron Microscope)

Transmission electron microscopy (TEM) creates images by passing a beam of electrons through a sample. The sample is usually prepared as an ultrathin section, typically under 100 nm thick, or as a suspension placed on a grid.

***In vitro* Drug Release Kinetics**

The drug release kinetics of the optimized nanogel formulation (F9) were analyzed using various kinetic models, such as zero-order, first-order, and Higuchi equations, derived from data obtained in in vitro release studies. The Korsmeyer-Peppas equation was used to analyze the drug release mechanism.

Zero-Order Kinetics

Cumulative amount of drug released was plotted against time.

$$C=K0t$$

In zero-order kinetics, the rate constant (K_o) is represented in units of concentration over time. Plotting concentration against time produces a straight line with a slope equal to K_o, indicating a constant drug release rate independent of concentration.

First Order Kinetics

In first-order kinetics, a graph is constructed by plotting the logarithm of the cumulative percentage of the remaining drug against time. This method explains drug release from formulations that rely on the drug's concentration.

$$Log\ C=Log\ Co+Kt/2.303$$

Where C0 is the initial concentration of drug, k is the first order constant, and t is the time.

Higuchi's Model

Higuchi's model involves plotting the cumulative percentage of drug release against the square root of time.

$$Q=Kt1/2$$

In the Higuchi model, the constant K represents the system's design variables, and t denotes time in hours. This model characterizes drug release based on Fickian diffusion, describing it as a process dependent on the square root of time from a swellable matrix.

Korsmeyer-Peppas Equations

The drug release mechanism was determined by analyzing the first 60% of the release data using the Korsmeyer-Peppas model. A log-log plot of the cumulative percentage of drug released versus time was created, and the release exponent (n) was derived from the slope of the resulting straight line.

$$Mt/M\infty=Ktn$$

In the Korsmeyer-Peppas model, the fraction of the drug released at time t is represented as MtM∞\frac{M_t}{M_\infty}M∞Mt, where MtM_tMt is the amount of drug released at time t, and M∞M_\inftyM∞ is the total drug released at infinite time. Constant K is a kinetic parameter specific to the drug-polymer system, while nnn is the release exponent that reveals the mechanism of drug release. The release process is influenced by factors such as polymer swelling, erosion, and diffusion through the hydrated matrix. The value of nnn helps to identify the specific diffusion mechanism:

- $n \leq 0.45$: This indicates Fickian diffusion (Case I), where the release is mainly controlled by diffusion.
- 0.45<n<0.890.45 < n < 0.890.45<n<0.89: Suggests non-Fickian (anomalous) diffusion, where both diffusion and polymer relaxation govern the release.
- n=0.89n = 0.89n=0.89: Corresponds to zero-order release (Case II transport), indicating a release rate independent of time, primarily involving polymer relaxation.
- When n>0.89n > 0.89n>0.89, it signifies super Case II transport, where the release mechanism is primarily governed by polymer relaxation and erosion.
- .

Comparison Drug Release Data with Formulated Nanogel and Marketed formulation

An in vitro release study was conducted to compare the optimized formulation with the marketed product.

RESULTS AND DISCUSSION

Pre-formulation Studies

Physical Characteristics

Acyclovir and omeprazole were evaluated for their physical characteristics, including color, odor, and texture. Both substances are white, odorless, and exhibit an amorphous powder form.

Melting Point

The melting point of acyclovir was measured using the capillary tube method and was found to be 256°C, which aligns with the literature value of 256.5°C.

The melting point of omeprazole was determined using the capillary tube method and found to be 156°C, consistent with the literature value of 156°C.

Solubility Studies

The solubility of acyclovir and omeprazole was evaluated in different solvents, such as water, methanol, ethanol, and a pH 7.4 buffer solution. Acyclovir was found to be only slightly soluble in water and methanol, but highly soluble in both ethanol and the pH 7.4 buffer. Conversely, omeprazole exhibited high solubility in methanol and ethanol, while being sparingly soluble in water and pH 7.4 buffer.

Determination of Standard Graph

A standard calibration curve was established using concentrations ranging from 2 to 10 μg/ml, with corresponding absorbance values recorded as detailed in Table 3. The correlation coefficient (r^2) was determined to be 0.9918, indicating a strong linear relationship.

Determination of Standard Graph

A standard calibration curve was established using concentrations ranging from 2 to 10 μg/ml, with corresponding absorbance values recorded in Table 4. The correlation coefficient (r^2) was determined to be 0.9872, indicating a strong linear relationship, as depicted in Figure 1.

Excipient Compatibility Studies

FT IR Study

A study was performed to evaluate the compatibility between the drug and excipients using Fourier Transform Infrared (FTIR) spectroscopy. The analysis revealed no incompatibilities between the drug and the excipients used in the formulation, as illustrated in Figures 2 and 3.

Table 3. Calibration data of Acyclovir.

S.N.	Calibration data	Absorbance at 251 nm
1	2	0.050
2	4	0.118
3	6	0.202
4	8	0.247
5	10	0.307

Acyclovir and Omeprazole Nanogel

Developing a nanogel that combines acyclovir, and omeprazole presents a promising strategy for concurrently addressing viral infections and gastric conditions. This advanced delivery system has the potential to enhance drug effectiveness, improve bioavailability, and reduce side effects, thereby offering a comprehensive treatment approach for patients with coexisting health issues.

Compatibility Study

The compatibility of the compounds was assessed using FTIR analysis, which identified the functional groups present in the formulations. The FTIR spectrum of Acyclovir API revealed NH, OH, CH, C–O, C=O, and C=N stretching at 3435.27, 3175.78, 2680.11, 1213.51, 1701.11, and 1628.54 cm^{-1},

respectively. For Acyclovir gel, the peaks at 3278.18, 1637.30, and 1410.26 cm^{-1} corresponded to OH, C=N, and C–O stretching.

Omeprazole API exhibited functional groups S=O, NH, C–O, and CN stretching at 1410.65, 1774.24, 1266.89, and 2945.42 cm^{-1}, respectively. Carbopol 940 showed peaks at 3324.56, 1700.59, and 2940.23 cm^{-1}, representing OH, C=O, and CH stretching. Similarly, triethanolamine displayed OH, C–N, and CH stretching at 3308.32, 1405.33, and 2945.60 cm^{-1}, respectively.

The combined formulation of Acyclovir and Omeprazole gel exhibited peaks at 3317.30, 1636.52, and 1043.79 cm^{-1}, corresponding to OH, C=N, and C–O stretching, respectively. While slight variations in peak positions were observed, they indicate compatibility between the components, supporting the development of an effective combinational formulation, as detailed in Table 5.

FORMULATION OF NANOGEL

The selection of polymers for formulating acyclovir and omeprazole via the emulsion solvent diffusion method was guided by trial batches utilizing various polymers, including carbopol, triethanolamine, and PPG. The drug-to-polymer ratios were determined based on existing literature. Among the formulations tested, F9 emerged as the most suitable for combining acyclovir and omeprazole, as detailed in Table 6.

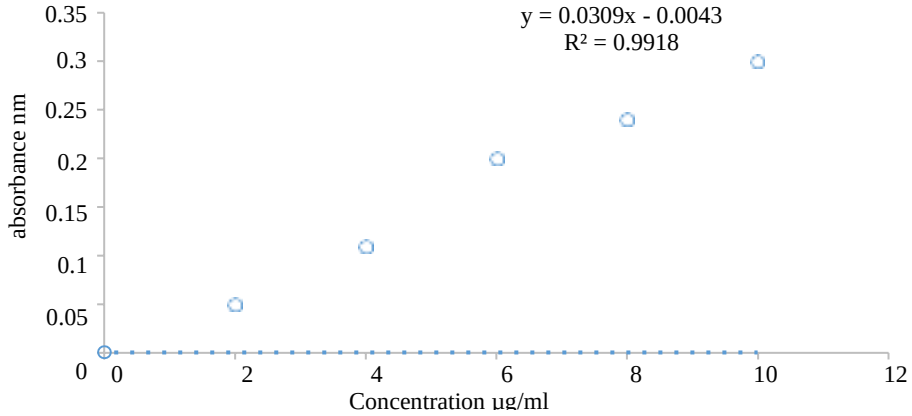

Figure 1. Standard graph curve of acyclovir.

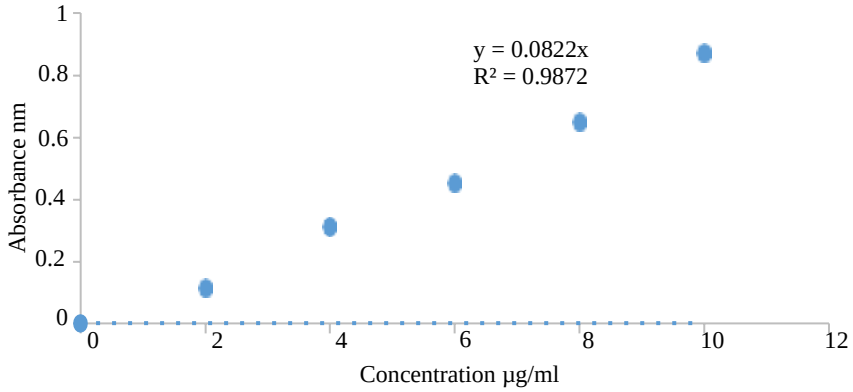

Figure 2. Standard graph of omeprazole.

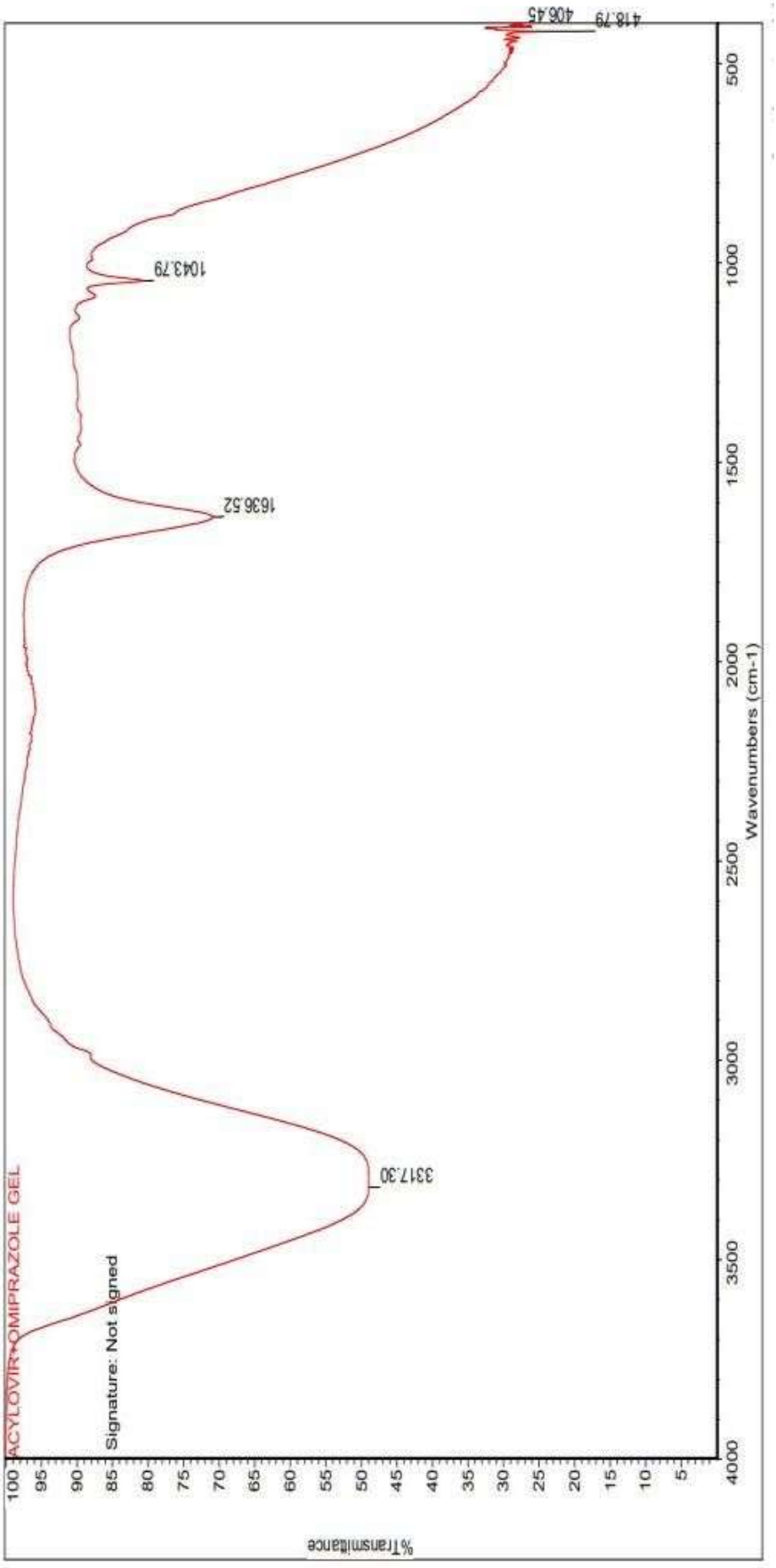

Figure 3. FT-IR of acyclovir and omeprazole nanogel.

Table 4. Calibration data of Omeprazole.

S.N.	Calibration data (µg/ml)	Absorbance at 305 nm
1	2	0.116
2	4	0.312
3	6	0.452
4	8	0.647
5	10	0.870

Table 5. FT-IR of acyclovir and omeprazole nanogel.

S.N.	Wave number cm^{-1}	Assignment
1	3317.30	OH stretching
2	1636.52	C=N stretching

Table 6. Trial batches for formulation of acyclovir and omeprazole.

Drug	Formulation code	Observed
Acyclovir and Omeprazole nanogel	F1	Light yellow
	F2	Solid in nature
	F3	Brown
	F4	Liquid in nature
	F5	Pale yellow
	F6	Pale orange
	F7	Semiliquid
	F8	Hard gel
	F9	transparent gel

CHARACTERISATION OF ACYCLOVIR AND OMEPRAZOLE NANOGEL

Determination of pH

The pH levels of formulations F1 through F9 varied, reflecting the differing polymer-to-drug ratios in each formulation.

Homogeneity

All gel formulations (F1–F9) exhibited excellent homogeneity, being free from lumps, particles, aggregates, foreign matter, and phase separation. The gels were transparent and demonstrated uniform consistency.

Spreadability

The spreadability diameters of formulations F1 through F9 indicated that the gels were easily spreadable.

Viscosity

The viscosity of each nanogel formulation was determined using a Brookfield viscometer. In this technique, a cone attached to a holding rod is dropped from a height of 10 cm, ensuring it falls directly into a glass cup containing the nanogel. The resistance the cone experiences as it moves through the gel is used to calculate the viscosity, which is reported in centipoise (cps).

Percentage Yield Analysis

Formulation F9 achieved the highest percentage yield at 96.02%, while formulation F2 had the lowest at 32%. These results indicate that F9 exhibits superior yield efficiency, as illustrated in Figure 4.

Drug Content

Formulation F9 exhibited the highest drug content at 92.65%, while formulation F2 had the lowest. Overall, the prepared nanogels demonstrated high drug entrapment efficiency, as detailed in Tables 7–9.

IN VITRO DRUG RELEASE STUDIES

The in vitro release profile of the acyclovir and omeprazole nanogel formulation was assessed using a cellophane membrane in a Franz diffusion cell. Drug release was tracked at different time intervals, and the results are presented in Figures 5–7.

In vitro release studies showed that out of the nine nanogel formulations containing acyclovir and omeprazole, F9 had the highest release rates, reaching 99% and 97.5%, respectively, after 24 hours, as depicted in Figure 8.

OPTIMIZATION OF ACYCLOVIR AND OMEPRAZOLE NANOGEL BY CHARACTERISATION

Characterization studies of the acyclovir and omeprazole nanogel formulations revealed that formulation F9 showed the best drug release properties, as outlined in Tables 10–13.

Table 7. Evaluation of formulated batches of nanogel.

Formulation code	pH	Homogeneity	Spreadibility	Viscosity
F1	6.1	Homogenous	2.5	3459
F2	6.3	Homogenous	3.5	3356
F3	6.2	Homogenous	2.9	3268
F4	6.5	Homogenous	3.4	3498
F5	6.2	Homogenous	2.6	3295
F6	6.3	Homogenous	2.9	3501
F7	5.9	Homogenous	3.2	3340
F8	6.4	Homogenous	2.8	3351
F9	6.9	Homogenous	3.5	3528

Table 8. Percentage yield of acyclovir and omeprazole nanogel.

S.N.	Formulation code	Percentage yield (%)
1	F1	65.76
2	F2	32.55
3	F3	34.14
4	F4	44.56
5	F5	68.89
6	F6	71.18
7	F7	86.80
8	F8	78.25
9	F9	96.02

Table 9. Drug content of acyclovir and omeprazole nanogel.

S.N.	Formulation code	Drug content (%)
1	F1	60.54
2	F2	29.00
3	F3	30.84
4	F4	40.55
5	F5	61.45
6	F6	65.78
7	F7	85.11
8	F8	75.24
9	F9	92.65

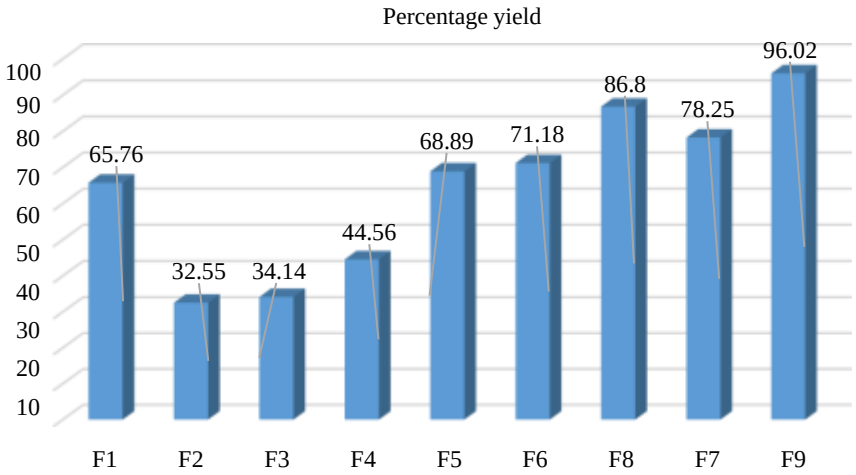

Figure 4. Percentage yield of acyclovir and omeprazole nanogel.

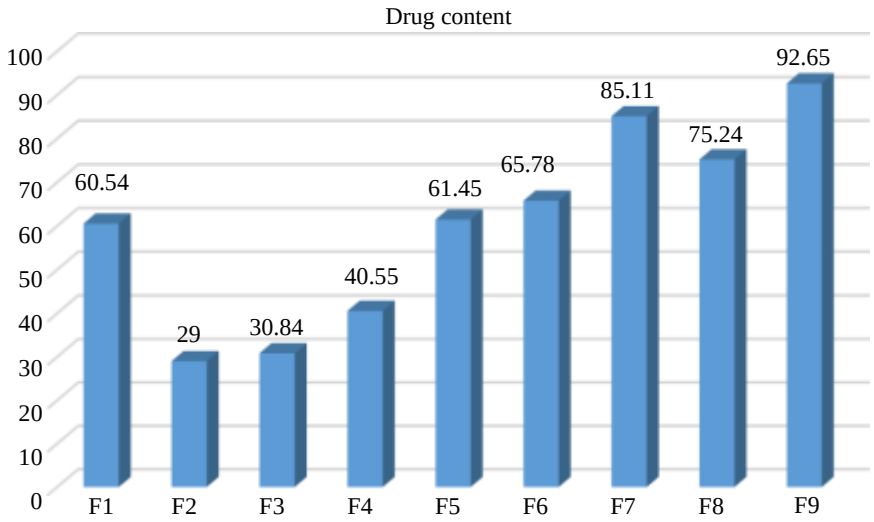

Figure 5. Drug content of acyclovir and omeprazole nanogel.

Table 10. *In vitro* drug release profile of acyclovir and omeprazole nanogel (F1–F3).

S.N.	Time (h)	Cumulative percentage drug release (%)					
		F1		***F2***		***F3***	
		A	*O*	*A*	*O*	*A*	*O*
1	0	0	0	0	0	0	0
2	1	3.4	0.5	1.2	1.1	1.5	1.5
3	2	12.5	9.5	8.8	7.2	10.6	8.8
4	4	25.2	20.8	24.5	15.4	18.7	17.3
5	6	43.8	35.1	40.5	27.9	29.3	23.9
6	8	53.6	50.5	50.9	43.5	35.6	39.6
7	12	60.4	55.7	55.3	51.4	42.1	46.4
8	16	65.5	60.8	60.4	69.6	56.6	52.5
9	20	79.9	70.0	62.9	72.3	65.2	65.7
10	24	80.1	75.9	70.4	75.7	72.7	69.1

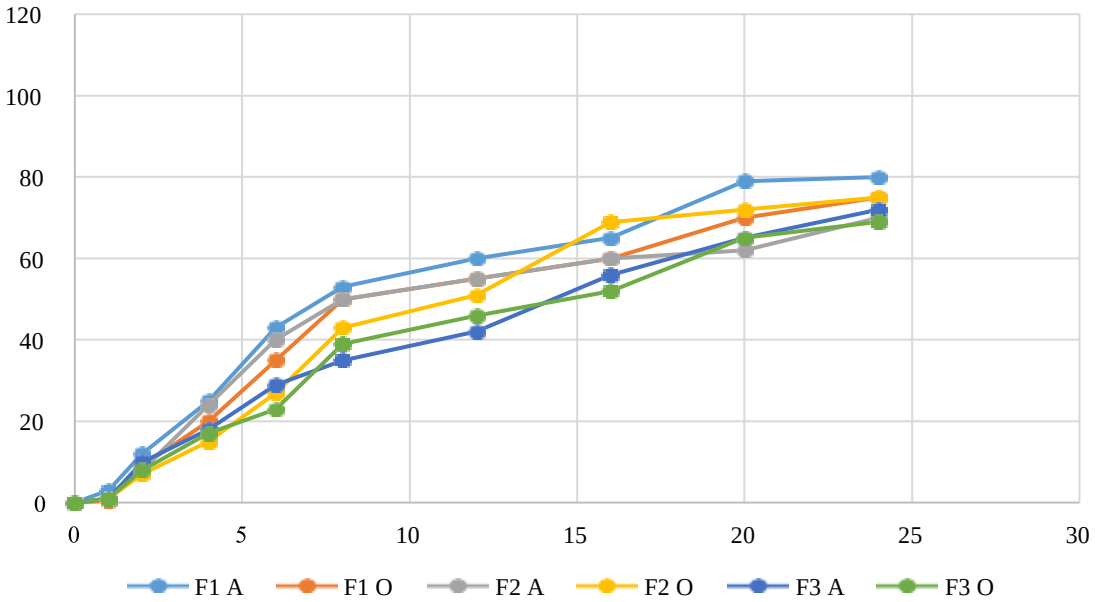

Figure 6. *In vitro* drug release profile of acyclovir and omeprazole nanogel (F1–F3).

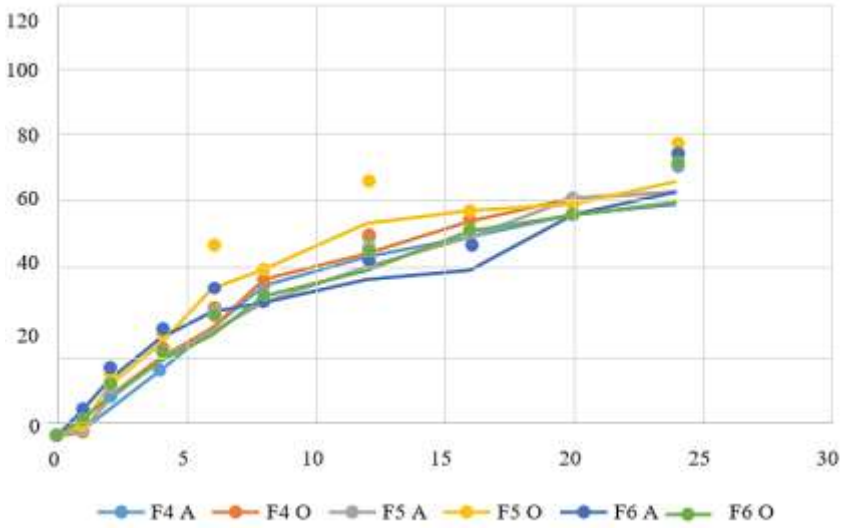

Figure 7. *In vitro* drug release profile of acyclovir and omeprazole nanogel (F4–F6).

Table 11. *In vitro* drug release profile of acyclovir and omeprazole nanogel (F4–F6).

S.N.	Time (h)	Cumulative percentage drug release (%)					
		F4		***F5***		***F6***	
		A	***O***	***A***	***O***	***A***	***O***
1	0	0	0	0	0	0	0
2	1	2.2	1.5	1.5	3.8	8.1	5.2
3	2	8.6	12.4	11.1	15.5	17.6	12.2
4	4	20.8	24.1	23.3	28.9	30.2	23.8
5	6	33.5	33.8	32.9	45.2	38.8	31.3
6	8	46.5	48.9	41.5	51.1	41.5	43.8
7	12	55.2	56.1	52.7	65.8	48.2	51.1
8	16	61.9	66.6	61.2	69.7	51.8	63.8
9	20	68.8	73.4	73.8	71.3	68.3	68.2
10	24	71.5	75.2	75.4	78.8	75.4	72.8

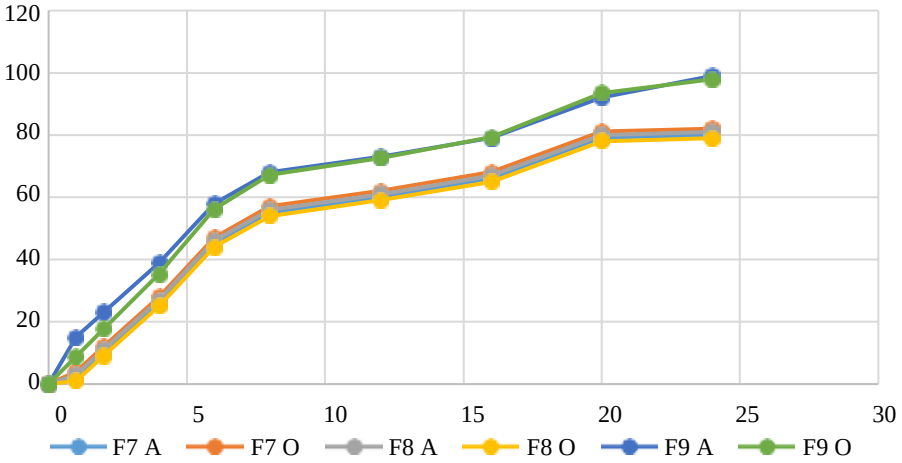

Figure 8. *In vitro* drug release profile of acyclovir and omeprazole nanogel (F7–F9).

Table 12. *In vitro* drug release profile of acyclovir and omeprazole nanogel (F7–F9).

S.N.	**Time (h)**	**Cumulative percentage drug release (%)**					
		F7		***F8***		***F9***	
		A	*O*	*A*	*O*	*A*	*O*
1	0	0	0	0	0	0	0
2	1	2.4	4.7	3.7	1.4	15.2	8.8
3	2	10.2	12.5	11.5	9.5	23.5	17.6
4	4	26.5	28.1	27.6	25.4	39.2	35.2
5	6	45.3	47.8	46.4	44.6	48.8	45.5
6	8	55.8	57.4	56.1	54.7	61.5	58.2
7	12	60.5	62.7	61.8	59.3	73.1	72.6
8	16	66.5	68.2	67.1	65.5	81.6	83.2
9	20	79.9	81.9	80.4	78.8	92.4	93.5
10	24	80.2	82.2	81.9	79.5	98.1	97.9

Table 13. Optimization of acyclovir and omeprazole nanogel by characterization.

S.N.	**Methods**	**Observed**	**Result**
1	pH	6.9	F9
2	Homogeneity	Homogenous	F9
3	Spreadability	3.5	F9
4	Viscosity	3528	F9
5	Percentage yield	96.02%	F9
6	Drug content	92.65%	F9
7	*In-vitro* dissolution study	99 (A)and 97.2(O)	F9

EVALUATION OF OPTIMIZED FORMULATED F9

Particle size and Zeta Potential

Particle size is a crucial factor in the characterization of nanogels. For formulation F9, dynamic light scattering analysis revealed an average particle size of 678.4 nm, with a polydispersity index (PDI) of 0.842 and an intercept of 0.857, as detailed in Table 14.

Determination of Zeta Potential

Zeta potential analysis, conducted using a Malvern Zetasizer, assesses the surface charge of nanoparticles to predict their colloidal stability during storage. Particles with zeta potential values exceeding +25 mV or below –25 mV typically exhibit high stability due to electrostatic repulsion, preventing aggregation. Conversely, low zeta potential values indicate insufficient repulsive forces, leading to particle flocculation.

The zeta potential of the acyclovir and omeprazole nanogel (formulation F9) was measured at –43.7 mV, with a peak area indicating 100% intensity. This significant negative zeta potential suggests that the nanogel possesses high colloidal stability, as illustrated in Figures 9 and 10.

TEM (Transmission Electron Microscope)

Transmission electron microscopy (TEM) creates images by directing a beam of electrons through a sample. The specimen is usually prepared as an ultrathin section, under 100 nm thick, or as a suspension placed on a grid.

***IN-VITRO* DRUG RELEASE KINETICS**

The in vitro release data of the acyclovir and omeprazole nanogel (F9) were examined to better understand the drug release mechanism. This involved fitting the data to various kinetic models, including zero-order kinetics, to identify the release pattern.

Table 14. Zeta potential of formulation F9.

S.N.	Formulation Code	Particle size	PDI	Zeta Potential
1.	F9	678.4	0.842	–43.7

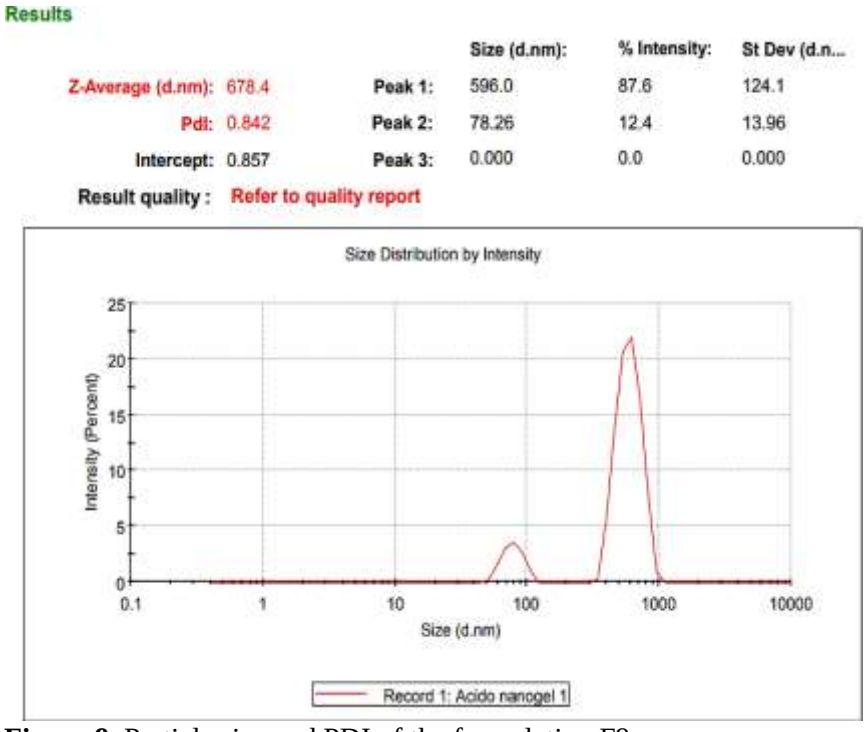

Figure 9. Particle size and PDI of the formulation F9.

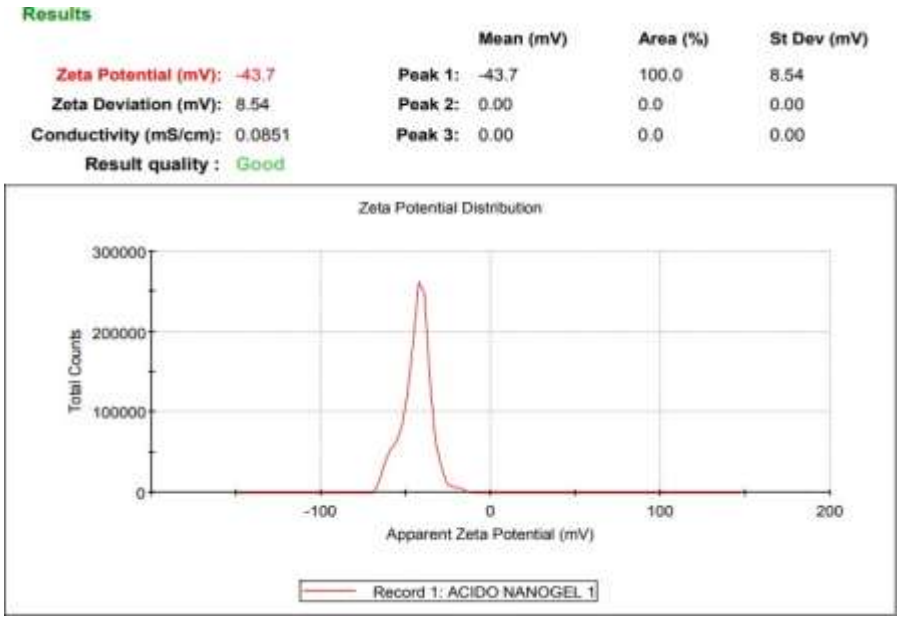

Figure 10. Zeta potential of formulation F9.

Figure 11. TEM image.

The optimal drug release mechanism was determined by evaluating the coefficient of determination (r^2) for the studied parameters, selecting the model with the highest r^2 value as the most appropriate fit. For the acyclovir and omeprazole nanogel formulation F9, the zero-order kinetic model exhibited the highest r^2 value, suggesting it as the most appropriate model. This was further confirmed by plotting the percentage cumulative drug release against the square root of time, yielding r^2 values between 0.928 and 0.921. However, in many experimental scenarios, drug diffusion deviates from Fickian behavior, displaying non-Fickian (anomalous) characteristics. In such cases, the Korsmeyer-Peppas model is employed to analyze release kinetics. Notably, formulation F9 adhered to Fick's law of diffusion, while the other formulations exhibited anomalous behavior, as illustrated in Figure 11.

SUMMARY

- The λmax values of acyclovir and omeprazole were confirmed using a UV spectrometer at 251 nm and 305 nm, respectively.
- A standard calibration curve was plotted for various concentrations of acyclovir and omeprazole.
- Acyclovir and omeprazole nanogel was successfully formulated using the solvent diffusion method.

- The pH of formulations (F1–F9) was measured, with F9 being identified as the most suitable for gel preparation.
- The drug content was assessed using UV spectroscopy.
- The prepared nanogels were opaque, free of lumps, particles, and aggregates, ensuring uniformity across all formulations.
- The spreadability test of F9 indicated excellent spreadability, with viscosities ranging from 3268 to 3528 cps, confirming the stability of the formulations.
- In vitro dissolution studies revealed that F9 demonstrated an exceptional dissolution rate.
- The particle size, polydispersity index (PDI), and zeta potential of F9 were measured, showing values of 687.4 nm, 0.842, and -43.7 mV, respectively.
- Transmission electron microscopy (TEM) images confirmed that the nanogel particles were spherical with a smooth surface, measuring approximately 650 nm in size.

Comparison of F9 Nanogel and Marketed Formulation (MF):

- In in-vitro release studies, the F9 nanogel formulation demonstrated greater efficiency compared to the marketed acyclovir ointment.
- The study concluded that the F9 nanogel provides sustained drug release, enhancing antiviral activity when compared to conventional formulations, emphasizing the potential of nanogel-based drug delivery systems.

CONCLUSION

The experimental study successfully developed a nanogel formulation combining an antiviral drug and an anti-ulcer drug, resulting in a product with a spherical, smooth surface and a nanoscale particle size. The nanogel was opaque, free of lumps, particles, and aggregates, ensuring homogeneity across all formulations. Among the tested formulations, F9 demonstrated superior drug content and an optimal particle size of less than 1000 nm, confirming its classification within the nanoscale range.

All nanogel formulations maintained a pH range of 6.1 to 6.9, with F9 exhibiting the highest pH of 6.9, which falls within the acceptable range for nanogels (1 to 7 pH). The spreadability study confirmed that F9 possesses excellent spreadability. The viscosity of the formulations ranged from 3268 to 3528 centipoise (cps), indicating their stability. Additionally, formulation F9 exhibited the highest drug release percentage among all tested formulations. In vitro diffusion studies demonstrated that F9 followed a controlled drug release pattern, highlighting its effectiveness.

Short-term stability tests confirmed that the formulation remained stable. Based on its outstanding morphological characteristics, efficient drug content, and controlled release profile, F9 was identified as the optimized formulation. It proved to be more effective than the marketed acyclovir ointment (ACIVIR), further underscoring its potential as an advanced drug delivery system.

REFERENCES

1. Paudel KS, Milewski M, Swadley CL, Brogden NK, Ghosh P, Stinchcomb AL. Challenges and opportunities in dermal/transdermal delivery. *Ther Deliv*. 2010; 1(1): 109–131.
2. Wright S, Yelland M, Heathcote K, Ng SK, Wright G. Fear of needles-nature and prevalence in general practice. *Aust Fam Physician*. 2009; 38(3): 172–176.
3. McMurtry CM, Pillai Riddell R, Taddio A, Racine N, Asmundson GJ, Noel M, Chambers CT, Shah V, HelpinKids, Adults Team. Far From "Just a Poke": Common Painful Needle Procedures and the Development of Needle Fear. *Clin J Pain*. 2015; 31: S3–S11.
4. Pastore MN, Kalia YN, Horstmann M, Roberts MS. Transdermal patches: history, development and pharmacology. *Br J Pharmacol.* 2015; 172(9): 2179–2209.

5. Waghule T, Rapalli VK, Gorantla S, Saha RN, Dubey SK, Puri A, Singhvi G. Nanostructured Lipid Carriers as Potential Drug Delivery Systems for Skin Disorders. *Curr Pharm Des.* 2020; 26(36): 4569–4579.
6. Silva SM, Hu L, Sousa JJ, Pais AA, Michniak-Kohn BB. A combination of nonionic surfactants and iontophoresis to enhance the transdermal drug delivery of ondansetron HCl and diltiazem HCl. *Eur J Pharm Biopharm.* 2012; 80(3): 663–673.
7. Pradhan M, Srivastava S, Singh D, Saraf S, Saraf S, Singh MR. Perspectives of Lipid-Based Drug Carrier Systems for Transdermal Delivery. *Crit Rev Ther Drug Carrier Syst.* 2018; 35(4): 331–367.
8. Araujo VHS, Delello Di Filippo L, Duarte JL, Sposito L, Camargo BAF, da Silva PB, Chorilli M. Exploiting solid lipid nanoparticles and nanostructured lipid carriers for drug delivery against cutaneous fungal infections. *Crit Rev Microbiol.* 2021; 47(1): 79–90.
9. Sguizzato M, Esposito E, Cortesi R. Lipid-Based Nanosystems as a Tool to Overcome Skin Barrier. *Int J Mol Sci.* 2021; 22(15): 8319.
10. Gupta M, Agrawal U, Vyas SP. Nanocarrier-based topical drug delivery for the treatment of skin diseases. *Expert Opin Drug Delivery*. 2012; 9(7): 783–804.
11. Qi T, Chen B, Wang Z, Du H, Liu D, Yin Q, Liu B, Zhang Q, Wang Y. A pH-Activatable nanoparticle for dual-stage precisely mitochondria-targeted photodynamic anticancer therapy. *Biomaterials*. 2019; 213: 119219.
12. Hui Y, Yi X, Hou F, Wibowo D, Zhang F, Zhao D, Gao H, Zhao CX. Role of Nanoparticle Mechanical Properties in Cancer Drug Delivery. *ACS Nano*. 2019; 13(7): 7410–7424.
13. Birrenbach G, Speiser PP. Polymerized micelles and their use as adjuvants in immunology. *J Pharm Sci.* 1976; 65(12): 1763–1766.
14. Yang L, Kwan CS, Zhang LL, Li XH, Han Y, Leung KCF, Yang YG, Huang ZF. Chiral Nanoparticle-Induced Enantioselective Amplification of Molecular Optical Activity. *Adv Funct Mater*. 2019; 29(8): 1807307.
15. Shchelokov A, Palko N, Potemkin V, Grishina M, Morozov R, Korina E, Uchaev D, Krivtsov I, Bol'shakov O. Adsorption of Native Amino Acids on Nanocrystalline TiO2: Physical Chemistry, QSPR, and Theoretical Modeling. *Langmuir*. 2019; 35(2): 538–550.
16. Rancan F, Volkmann H, Giulbudagian M, Schumacher F, Stanko JI, Kleuser B, Blume-Peytavi U, Calderon M, Vogt A. Dermal Delivery of the High-Molecular-Weight Drug Tacrolimus by Means of Polyglycerol-Based Nanogels. *Pharmaceutics*. 2019; 11(8): 394.
17. Rancan F, Asadian-Birjand M, Dogan S, Graf C, Cuellar L, Lommatzsch S, Blume-Peytavi U, Calderon M, Vogt A. Effects of thermoresponsivity and softness on skin penetration and cellular uptake of polyglycerol-based nanogels. *J Control Release*. 2016; 228: 159–169.
18. Tiwari N, Osorio-Blanco ER, Sonzogni A, Esporrin-Ubieto D, Wang H, Calderon M. Nanocarriers for Skin Applications: Where Do We Stand? *Angew Chem Int Ed Engl.* 2022; 61(3): e202107960.
19. Ratemi E, Sultana Shaik A, Al Faraj A, Halwani R. Alternative approaches for the treatment of airway diseases: focus on nanoparticle medicine. *Clin Exp Allergy*. 2016; 46(8): 1033–1042.
20. Yau A, Lee J, Chen Y. Nanomaterials for Protein Delivery in Anticancer Applications. *Pharmaceutics*. 2021; 13(2): 155.

